Adsorption Selectivity of Benzene/Propene Mixtures for Various Zeolites

Shuai Ban,[†] Adri van Laak,[‡] Petra E. de Jongh,[‡] Jan P. J. M. van der Eerden,[†] and Thijs J. H. Vlugt*[,†]

Condensed Matter and Interfaces, Department of Chemistry, Utrecht University, P.O. Box 80.000 3508 TA Utrecht, The Netherlands, and Inorganic Chemistry and Catalysis, Department of Chemistry, Utrecht University, P.O. Box 80.000 3508 TA Utrecht, The Netherlands

Received: June 24, 2007; In Final Form: September 10, 2007

The nine-site benzene model of Zhao et al. (*J. Phys. Chem. B* **2005**, *109*, 5368−5374) has been used to systematically study the adsorption of benzene, propene, and benzene−propene mixtures in zeolites mordenite, Y, β, silicalite, and MCM22. Interaction parameters for the benzene−zeolite interactions have been fitted to available adsorption experiments from literature. As an independent check of our force field, we have performed additional adsorption experiments using the TEOM technique and excellent agreement between simulations and TEOM experiments was found. High adsorption selectivities for benzene in benzene−propene mixtures were found in all zeolites, except for silicalite.

1. Introduction

Cumene (isopropylbenzene) is an important chemical intermediate used for the production of phenol and acetone.[1] Traditional cumene production is based on the alkylation of benzene and propene using a solid acid catalyst. This process requires a large excess of benzene (high benzene/propene (B/P) ratio) to suppress side reactions, for example, alkene oligomerization and multiple alkylations of benzene. In alkylation processes, a high ratio of "inert" reactant (e.g., benzene) versus reactive reactant molecules (e.g., alkenes) can be realized by a proper selection of the reactor type.[2] The large size of reactors, separation units, and recycling streams of production plants due to the large excess of benzene brings about both large energy consumption and high capital investments.[3]

There is a large interest to replace the solid acid catalyst for cumene production by protonated zeolites. This could have the following advantages: (1) a lower operating temperature, which results in less byproducts and (2) the possibility of reducing the B/P ratio.[2] In the ideal situation, the B/P ratio is only very large at the active site inside the zeolite and close to one in the reactor feed. Promising results for the production of cumene have been found for the zeolites mordenite, Y, β, and MCM22.[3]

Understanding of the adsorption and diffusion of benzene and propene at the molecular scale is necessary in order to optimize such processes. In this work, molecular simulations are used to investigate the location and the adsorption thermodynamics of propene and benzene in various zeolites. The adsorption of linear alkanes in zeolites has been well studied by experiments[4−9] and Monte Carlo simulations.[10−20] The adsorption and diffusion of alkenes is not well accessible through experiments because of their reactivity.[17,21] The first Monte Carlo simulations of benzene in zeolites were performed by Snurr et al.[22] using an all-atom model with 12 charged sites (similar to the OPLS model for benzene[23]). This model has been used extensively.[24−26] Recently, it has been found that a correct representation of the quadrupole moment (originating from the π system of benzene) is crucial for the reproduction of the structure of liquid and solid benzene.[27,28] In particular, the orientation dependence of the interaction between benzene molecules (often a T-shaped structure[29−31]) strongly depends on the quadrupole moment.[27,28] Note that the OPLS model for benzene has no quadrupole moment. Siepmann and co-workers have introduced a nine-site model for benzene[28,32] in which the CH groups are modeled as chargeless united atoms and three additional charged interaction sites are added to reproduce the quadrupole moment caused by the π system. This model correctly reproduced the experimental vapor−liquid and vapor−solid phase coexistence as well as the sublimation and evaporation pressures. Because the 9-site model

TABLE 1: Zeolites Used in This Study[a]

framework[a]	number of unit cells	size of simulation box [Å]	space group
MOR	$2 \times 2 \times 5$	$36.188 \times 41.032 \times 37.620$	*Cmcm*
MFI	$2 \times 2 \times 3$	$40.044 \times 39.798 \times 40.149$	*Pnma* (ortho)
MFI	$2 \times 2 \times 3$	$40.242 \times 39.640 \times 40.314$	$P2_12_12_1$ (para)
FAU	$1 \times 1 \times 1$	$25.028 \times 25.028 \times 25.028$	$Fd-3m$
BEA	$2 \times 2 \times 1$	$25.322 \times 25.322 \times 26.406$	$P4_122$
MWW	$1 \times 2 \times 1$	$24.447 \times 28.228 \times 24.882$	$P6/mmm$

[a] Framework types: mordenite (MOR), silicalite (MFI), Y (FAU), β (BEA), and MCM22 (MWW). The coordinates of the atoms of *para*-MFI are taken from van Koningsveld et al.[37] The atomic positions of the other frameworks have been taken from ref 38.

TABLE 2: Lennard-Jones Parameters for Guest−Guest and Guest−Host Interactions[a]

molecule	atom type	σ [Å]	ϵ/k_B [K]
propene	CH_3-CH_3	3.76	108.0
	$CH_2(sp2)-CH_2(sp2)$	3.68	92.5
	$CH(sp2)-CH(sp2)$	3.73	52.0
	CH_3-O	3.48	93.0
	$CH_2(sp2)-O$	3.50	82.6
	$CH(sp2)-O$	3.43	69.0
benzene	$CH_{benzene}-CH_{benzene}$	3.74	53.5
	$CH_{benzene}-O$	3.38	73.0

[a] LJ interactions between Si and CH_x are not taken into account. Interaction parameters for non-identical hydrocarbon groups are calculated using the Jorgensen mixing rules.[40]

* Corresponding author. E-mail: t.j.h.vlugt@tudelft.nl.
[†] Condensed Matter and Interfaces.
[‡] Inorganic Chemistry and Catalysis.

10.1021/jp074918p CCC: $37.00
Published on Web 10/26/2007

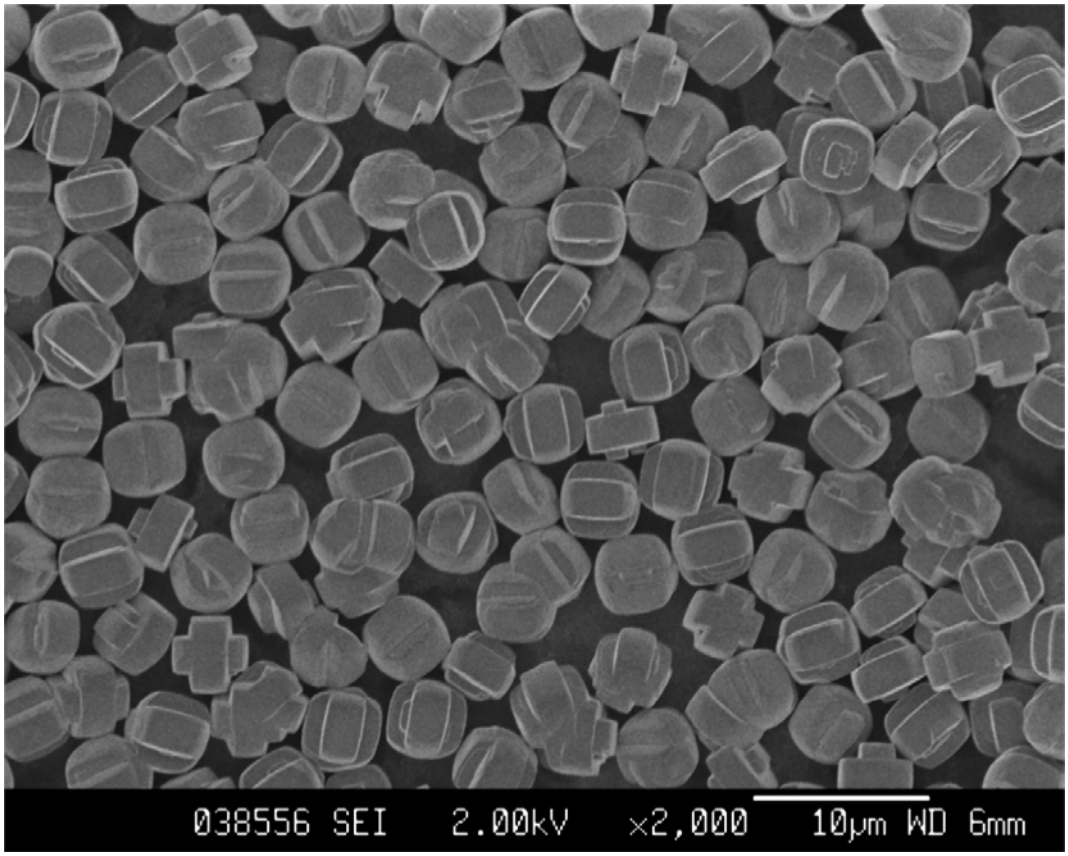

Figure 1. SEM image of our silicalite sample.

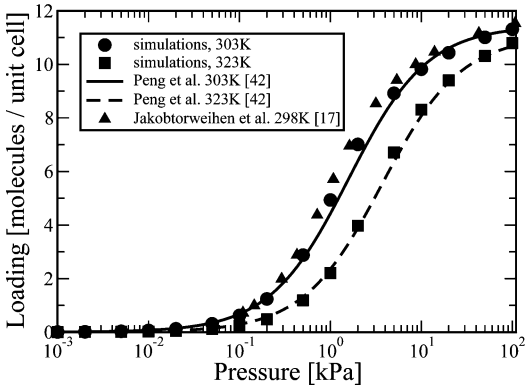

Figure 2. Experimental[42] and simulated[17] adsorption isotherms for propene in silicalite at various temperatures.

contains only 3 partial charges, it is computationally much more efficient than the 12-site model (12 partial charges).

In this work, we used this nine-site model to study the adsorption of benzene in various all-silica zeolites, that is, mordenite, Y, β, silicalite, and MCM22. We fitted the benzene−zeolite interactions to available experimental adsorption data (heats of adsorption and adsorption isotherms) from literature following the procedure of Dubbeldam et al.[15] We have also performed adsorption experiments as an independent check that our force field is able to reproduce the adsorption behavior of benzene. Our model is further used to calculate mixture isotherms and $x-y$ diagrams for benzene and propene. In particular, we find a high adsorption selectivity of benzene for mordenite, β, and MCM22, a slightly reduced selectivity for zeolite Y, and almost no selectivity for silicalite.

2. Methods

2.1. Simulation Method. Adsorption isotherms are calculated using figurational-bias Monte Carlo (CBMC) simulations in grand-canonical ensemble (GCMC).[11,33−35] In our simulations, Lennard-Jones (LJ) interactions are used to describe interactions between all adsorbates and zeolite atoms. The Ewald summation is used for Coulombic interactions between benzene and the zeolite. All other intermolecular interactions are truncated and shifted at 12 Å.[15] Periodic boundary conditions are applied. In our simulations, the pressure varies from 1.0 Pa to 1.0 bar, and temperatures range from 373 to 523 K. Under these conditions, pure benzene and propene are in the gas phase.

A typical simulation consists of at least 10^6 cycles. In each cycle, trial moves are attempted to translate, rotate, or (partially) regrow a molecule, to exchange a molecule with the reservoir, and to change the identity of a molecule (only for mixtures).[11] The number of trial moves per cycle is equal to the number of molecules with a minimum of 20. The parameters for the benzene−zeolite interactions were obtained using the procedure outlined by Dubbeldam et al.[15] using experimental isotherms for loadings up to the inflection point of benzene. Heats of adsorption are determined from isotherms using the Clausius−Clapeyron equation[36]

$$Q = -R\left(\frac{\partial \ln P/P_0}{\partial T^{-1}}\right)_{q=\text{constant}} \quad (1)$$

where P is the pressure, P_0 is an arbitrary reference pressure, T is the absolute temperature, q is the loading, and R is the gas constant.

The zeolites listed in Table 1 are studied as potential catalysts for cumene synthesis by computing the adsorption properties of propene and benzene. For silicalite, two frameworks with

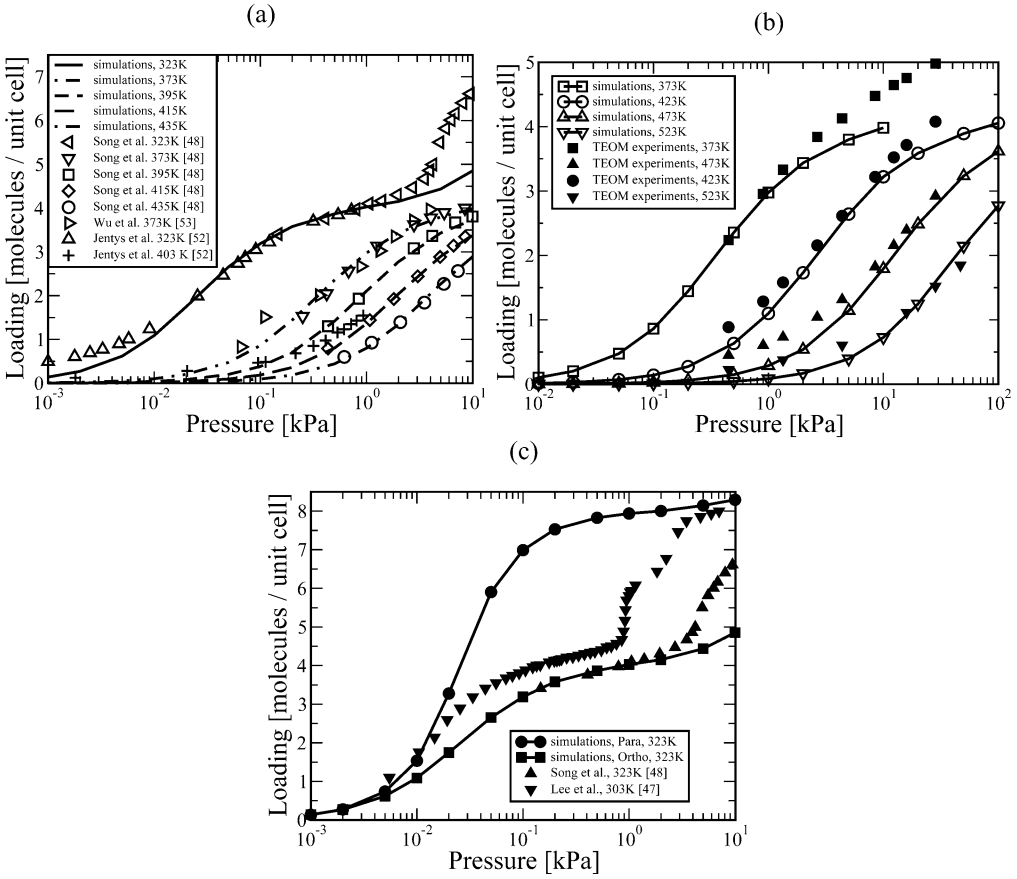

Figure 3. (a) Experimental[48,52,53] and simulated adsorption isotherms of benzene in silicalite (ortho structure) at various temperatures. The lines represent simulation data, and symbols are used for experiments. (b) Comparison between adsorption isotherms measured using the TEOM technique and simulations (ortho structure). (c) Simulated adsorption isotherms for benzene in *para* and *ortho*-silicalite at 323 K. The experimental isotherms of Song et al.[48] at 323 K and Lee et al.[47] at 303 K are shown for comparison.

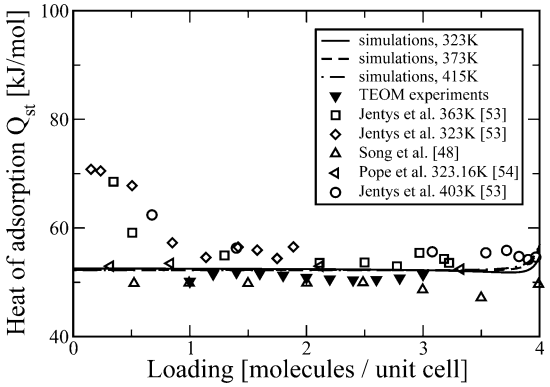

Figure 4. Experimental[48,54,53] and computed isosteric heats of adsorption of benzene in silicalite at various temperatures. The lines represent simulation data, and symbols are used for experimental data.

different space groups (ortho and para) are considered. In experiments, the transition from ortho to para is caused by the enlargement of the micropores during the adsorption of bulky aromatic molecules (see ref 25 for a discussion on this topic). In our simulations, this transition was not considered and either the ortho or para structure was simulated. We use a rigid approximation of zeolites, which is justified by the fact that flexibility results in only very small deviations of adsorption properties such as adsorption isotherms and Henry coefficients.[39]

2.2. Interaction Model. In Table 2, the Lennard-Jones parameters for the intermolecular interactions are listed. Propene is described by an uncharged united atom model. The parameters for the CH_3-CH_3 and CH_3-O interactions are taken from Calero et al.[16] The other interaction parameters for propene (LJ interactions, bond bending, and bond stretching) originate from Jakobtorweihen et al.[17] Note that Jakobtorweihen et al. used tail corrections and a different cutoff radius (14 Å). We have converted the original parameters of Jakobtorweihen et al. to a potential that is truncated and shifted at 12 Å without the use of tail corrections.

For benzene, the nine-site model of Zhao et al.[28] is used. Besides the six (uncharged) united CH atoms, three additional beads are used to model the quadrupole moment of benzene. These charged beads are located symmetrically on the sixfold axis with a positive charge of $+2.42e$ placed in the benzene plane and two compensating negatively charged beads at distances of 0.785 Å. Only the united CH atoms of benzene have LJ interactions with the zeolite or other guest molecules. The LJ interactions of benzene are adjusted to a potential that is truncated and shifted at 12 Å without the use of tail corrections. The partial charges of the zeolite atoms ($q_O = -1.025e$, $q_{Si} = +2.05e$) are taken from Calero et al.[16]

2.3. Experiments. Silicalite (ZSM5-06) was provided by ExxonMobil and consisted of intergrown x-shaped crystals with a uniform particle size of $\sim 4\ \mu$m, having a silica to alumina ratio of 600 in the gel (Figure 1). The silicalite was calcined in flowing air to remove template molecules by heating to 823 K at a rate of 0.83 K min^{-1} and was maintained at that temperature for 4 h before cooling down to ambient temperatures. A micropore volume of 0.14 $cm^3\ g^{-1}$ was recorded using N_2 physisorption (Micromeritics Tristar 3000) at 77 K.

Adsorption isotherms of benzene in MFI were recorded in a TEOM reactor (Rupprecht & Pataschnick TEOM 1500 PMA). The sample (approximately 65 mg) was transferred into a 100

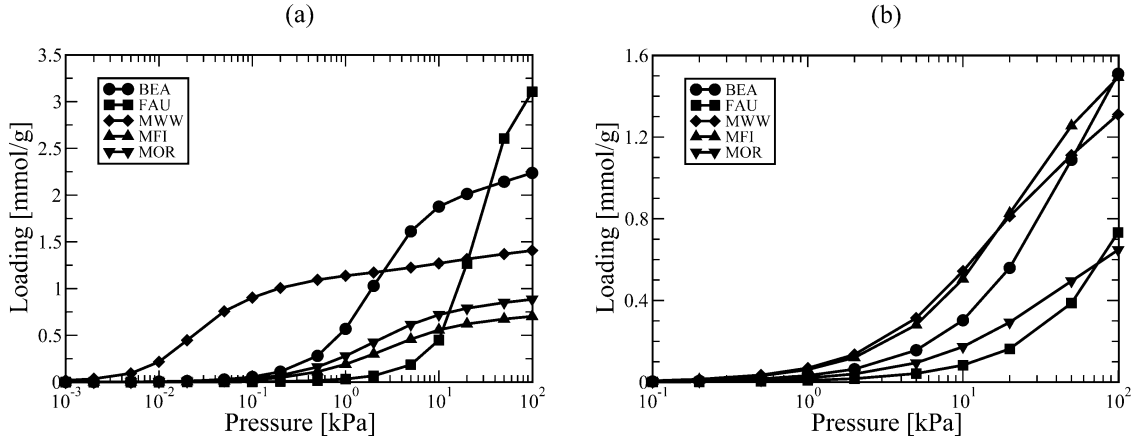

Figure 5. Simulated adsorption isotherms of (a) benzene at 423 K and (b) propene at 373 K in zeolite β (BEA), Y (FAU), MCM22 (MWW), silicalite (MFI), and mordenite (MOR).

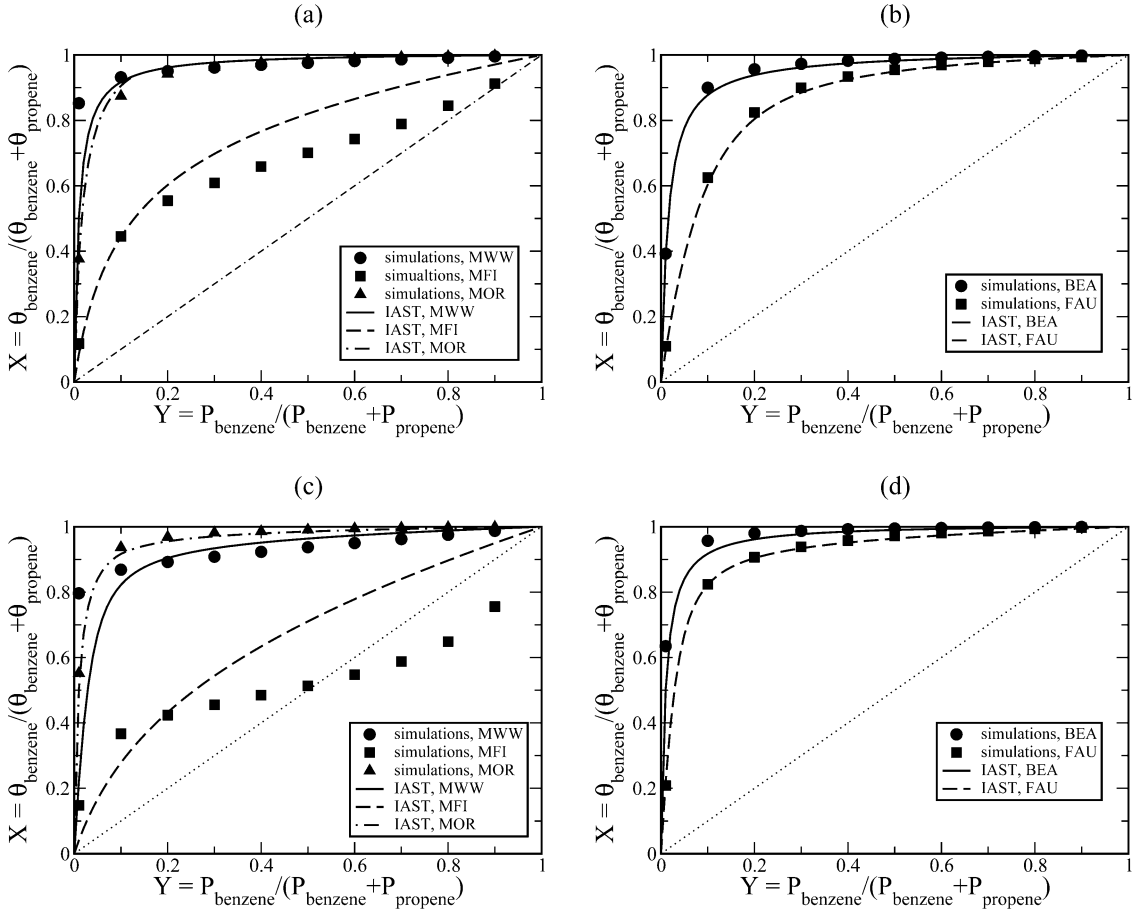

Figure 6. $x-y$ diagrams of benzene/propene mixtures in various zeolites (abbreviations as in Figure 5) at 423 K (a and b) and 373 K (c and d). Molecular simulations are compared with the IAST. Total pressure $P_{benzene} + P_{propene} = 1.0$ bar. θ_i and P_i denotes, respectively, the loading and partial pressure of component i. The dashed line is the expected result for a-selective adsorption.

μL quartz container and held in place between two layers of quartz wool. The sample was dried overnight at 623 K in situ in nitrogen atmosphere (grade 5.0). For measurements, helium (grade 4.6) was used as a carrier gas at a total pressure of 1.3 bar. Benzene was injected into the system using an ISCO 260D syringe pump in a range varying between 1 and 80 μL min^{-1} of benzene (Acros p.a.) in a helium flow of 80 mL min^{-1}, resulting in a benzene partial pressure between 0.45 and 46.8 kPa. Results were corrected for loss of water and changes in gas density. For a detailed description of the TEOM technique, we refer to Chen et al.[41] and Zhu et al.[6]

3 Results and Discussion

3.1. Adsorption of Pure Components. Figure 2 shows that our simulations for propene in silicalite agree well with experimental data at 303 and 323 K. As expected, we exactly reproduce the simulations of ref 17 from which our force field was derived. The heat of adsorption from our simulations is approximately 38.8 kJ/mol while experiments show a value of 40 kJ/mol.[43] Propene is absorbed both at the intersections and at the channel interiors of silicalite.

It is well known that benzene is a strong adsorbate with a large kinetic diameter of approximately 5.8 Å.[44] Therefore, in

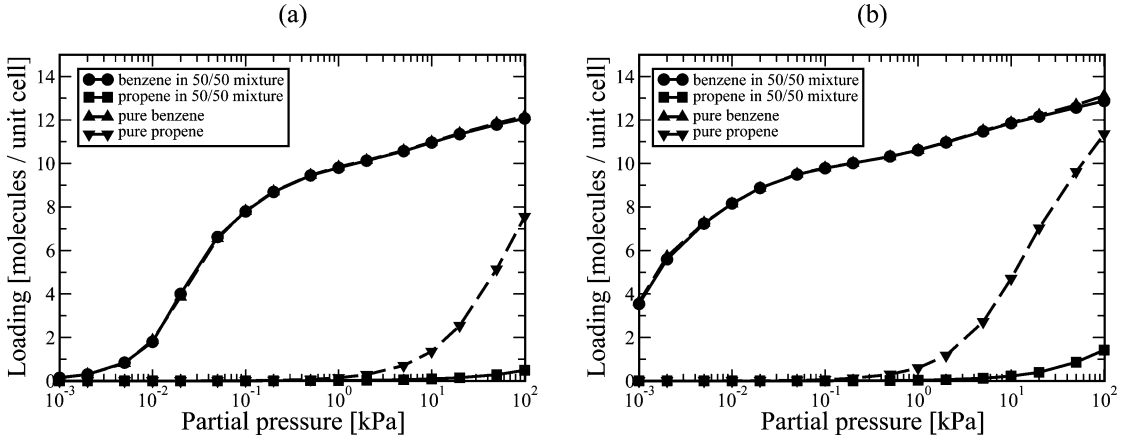

Figure 7. Adsorption isotherms of benzene and propene in equimolar (50/50) mixtures comparing with those of pure components in zeolite MCM22 at (a) 423 K and (b) 373 K.

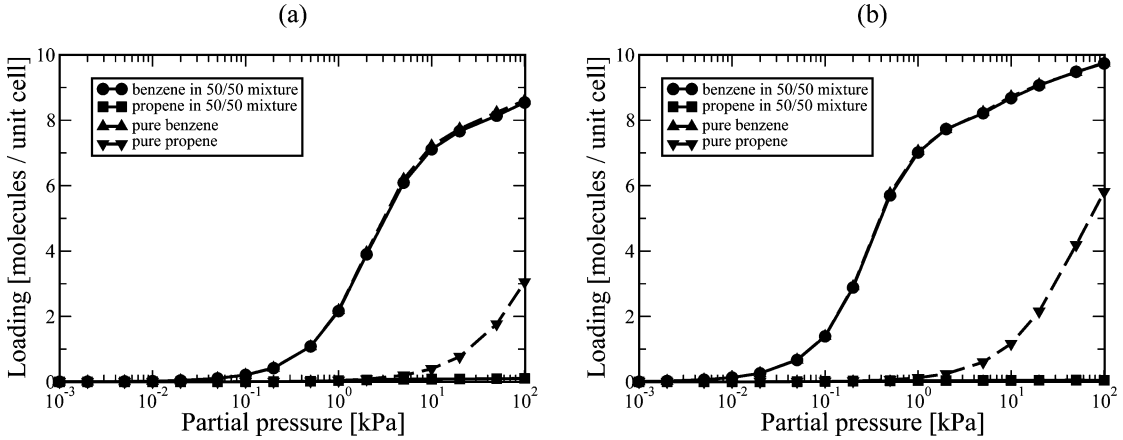

Figure 8. Adsorption isotherms of benzene and propene in equimolar (50/50) mixtures comparing with those of pure components in zeolite β at (a) 423 K and (b) 373 K.

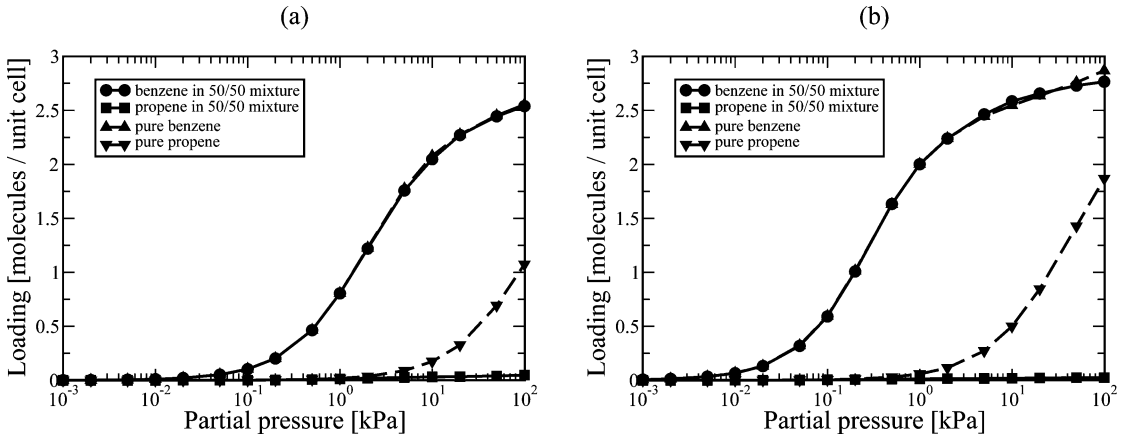

Figure 9. Adsorption isotherms of benzene and propene in equimolar (50/50) mixtures comparing with those of pure components in zeolite MOR at (a) 423 K and (b) 373 K.

silicalite, benzene is preferentially adsorbed at the relatively wide channel intersections (about 9 Å wide) instead of the channel interiors (straight channels of size 5.3 × 5.6 Å and zigzag channels of size 5.1 × 5.5 Å). Experiments[45−48] show that adsorption isotherms of aromatics (e.g., benzene, *p*-xylene) in silicalite have a characteristic inflection around four molecules per unit cell, which corresponds to the four channel intersections per unit cell in silicalite. NMR experiments[49,50] suggest that at four molecules per unit cell the silicalite framework gradually undergoes a transformation from space group ortho to para. At loadings below four molecules per unit cell, only the ortho structure is present, whereas at loadings larger than seven molecules per unit cell the para structure is found exclusively. An extra driving force is needed to push benzene molecules into the less-favorable channel interiors of silicalite. This process triggers the phase transition from ortho to para and results in an inflection in the adsorption isotherm. A similar inflection behavior (without a change in zeolite structure) has been found for branched hydrocarbons in MFI (e.g., isobutane).[51]

Figure 3a shows a comparison between our computed adsorption isotherms for benzene in ortho silicalite and the available experimental data. Only the experimental data of Figure 3a was used to fit the missing force field parameters of Table 2 and only up to the inflection point. Excellent agreement

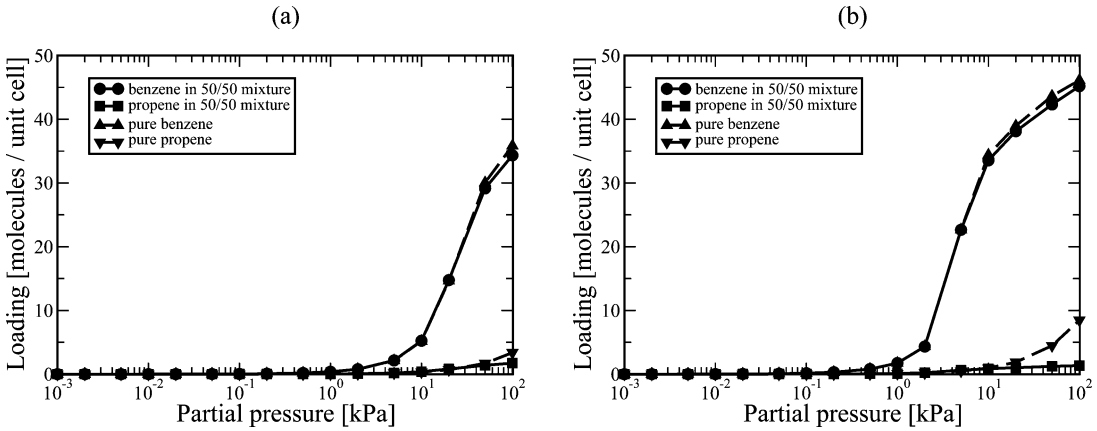

Figure 10. Adsorption isotherms of benzene and propene in equimolar (50/50) mixtures comparing with those of pure components in zeolite Y at (a) 423 K and (b) 373 K.

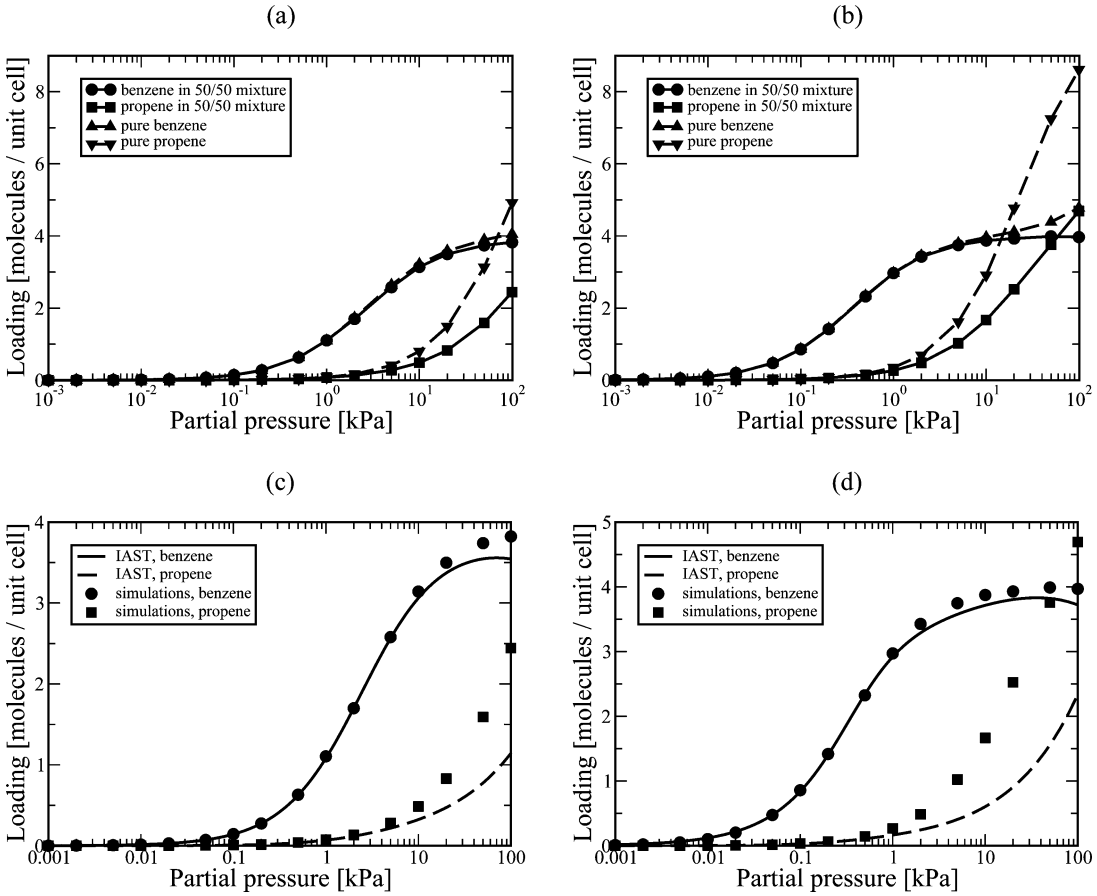

Figure 11. Adsorption isotherms of benzene and propene in equimolar (50/50) mixtures comparing with those of pure components in zeolite MFI at (a) 423 K and (b) 373 K. Comparison of the computed mixture isotherms (50/50 mixtures) with the IAST is shown in (c) 423 K and (d) 373 K.

is found for all simulations with loadings up to four molecules per unit cell. The isotherm of Song et al.[48] at 323 K deviates significantly at loadings higher than four molecules per unit cell. This suggests that beyond four benzene molecules per unit cell the structural transition of the frameworks needs to be taken into account. A comparison between our simulations and TEOM experiments is presented in Figure 3b. Excellent agreement is found at loadings lower than four benzene molecules per unit cell. Remarkably, the TEOM experiments at 373 K do not show the inflection behavior at four molecules per unit cell that was found in other experiments at much lower temperatures (323 K and lower). Note that to the best of our knowledge there is no experimental adsorption data available in literature at pressures required for such a possible inflection at 373 K. The maximum loading from the experiments agrees well with the computed maximum loading for the para structure (eight molecules per unit cell), see Figure 3c. In the para structure, benzene is still preferentially adsorbed at the channel intersections but adsorption in the channel interiors is also possible. The adsorption isotherm of benzene in the para structure does not show inflection behavior at four molecules per unit cell.

The isosteric heat of adsorption of benzene in silicalite is shown in Figure 4. Below a loading of four molecules per unit cell, simulations show a constant value of 52 kJ/mol, which is in line with experiments. However, at almost zero coverage, the heat of adsorption of Jentys et al.[53] is significantly higher (70 kJ/mol) and drops quickly with increasing loading. Jentys et al. explained this phenomenon by strong interactions of

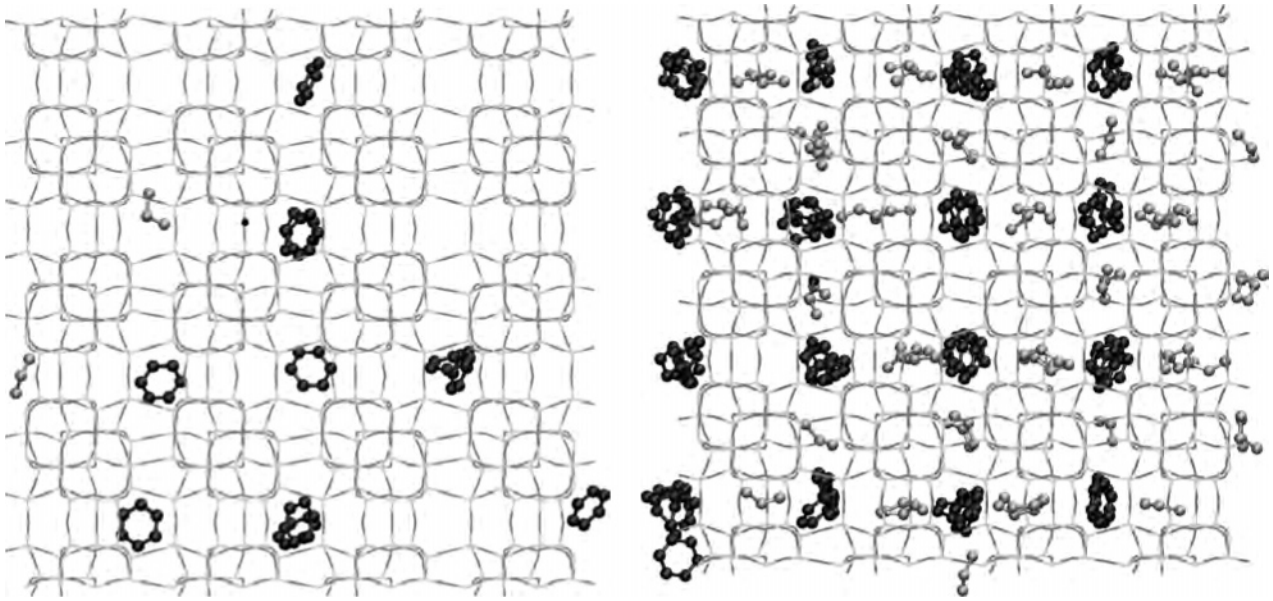

Figure 12. Typical snapshots of 50/50 benzene/propene mixtures at low (a) and high (b) total loading.

benzene with defect sites (e.g., SiOH groups), present in silicalite at very low concentrations. Indeed, at low pressure the isotherms from Jentys et al. overestimate our computed isotherms (see Figure 3a).

Takahashi and co-workers[55] have measured adsorption isotherms for benzene in FAU-type zeolite with a Si/Al ratio of 195. From their isotherms at 393 and 363K, we deduct $Q = 33$ kJ/mol and a Henry coefficient K_H (393 K) = 0.10 mmol g^{-1} Pa^{-1}. Because their data show a good comparison with our simulation results ($Q = 37$ kJ/mol and K_H (393 K) = 0.080 mmol g^{-1} Pa^{-1}), we are confident that our benzene force field is suitable for frameworks other than MFI.

Figure 5 shows the adsorption isotherms of benzene and propene in various all-silica frameworks. Mordenite consists of large straight channels (diameter 7 Å) and small side pockets (3.4 × 4.8 Å) that can be entered from the straight channels. At the temperatures and pressures in this study, benzene and propene are exclusively adsorbed in the straight channels. The adsorption for benzene starts at much lower pressures than those for propene because the attractive interactions of benzene with the framework are much stronger. The maximum loading of propene (in molecules per unit cell) is almost a factor of 3 larger than that of benzene. Zeolite Y is the most-open zeolite and consists of 12-Å-wide supercages accessible through 7.2-Å windows. This results in a low Henry coefficient and very high maximum loading. Zeolite MCM22 consists of two independent pore systems of 10-membered rings, a large cavity (7.1 × 18.0 Å), and a channel (4.0 × 5.5 Å). The cylindrical cavities of MCM22 are much smaller than the more sphere-like cavities of zeolite Y. Because the size of benzene is commensurate with the size of the cavity in MCM22, the Henry coefficient (slope of the adsorption isotherm at low loading) is very large.

3.2. Adsorption of Binary Propene/Benzene Mixtures. The $x-y$ diagrams of benzene/propene mixtures at a total pressure of 1 bar are plotted in Figure 6. A comparison with the Ideal Adsorbed Solution Theory (IAST) of Myers and Prausnitz[56] has been included. Three different types of adsorption behavior can be distinguished. Frameworks BEA, MWW, and MOR have very high selectivities for benzene. In these frameworks, propene and benzene are adsorbed at the same location in the zeolite. Because benzene is adsorbed much stronger than propene, the selectivity is very high. Because framework FAU has very large cavities, the benzene/propene selectivity is lower and close to the selectivity that one would expect for a liquid. The selectivity for benzene is even lower for framework MFI, and for $T =$ 373 K a reversal of the selectivity is observed. We will come back to this issue at the end of this section. The comparison with the IAST is quite good in general except for MFI because of the segregated nature of the adsorbed phase.[12,57]

As can seen from Figure 7, MCM22 is a strong absorbent for benzene. Large amounts of benzene are adsorbed at low pressures (around 1.0 Pa). The adsorption of benzene is hardly affected by propene, and therefore the pure component and mixture isotherms for benzene are identical. In the benzene/propene mixture, propene is excluded from the zeolite because benzene is adsorbed much stronger than propene. Because of the presence of the (narrow) channel system in MCM22 (4.0 × 5.5 Å), a small amount of propene is absorbed in these channels at low temperature. These channels are too small for benzene. The adsorption of propene in the narrow channel system directly results in a lower selectivity for benzene at 373 K (Figure 6b).

A similar feature is found for zeolites β and MOR (Figures 8 and 9) that almost exclusively adsorb benzene, independent of temperature. Figure 10 shows the somewhat weaker adsorption of benzene and propene in zeolite Y. At 423 K, the adsorption of benzene starts at 10 kPa and increases quickly with pressure. Therefore, the adsorption of benzene in zeolite Y is quite sensitive to pressure and this also leads to a lower selectivity for benzene at low partial pressures (Figure 6). This effect disappears at higher partial pressures of benzene. At low partial pressures of benzene, the benzene selectivity in zeolite Y depends more strongly on temperature than the other zeolites (MCM22, MOR, BEA, see Figure 6). The reason for this is that the adsorption isotherm of benzene in FAU is very sensitive to the pressure. Changes in the temperature effectively shift adsorption isotherms, and therefore the benzene loading can change significantly with temperature.

The adsorption of benzene/propene mixtures is significantly different in MFI because propene is not excluded from the zeolite, see Figure 11. Instead, the adsorption of propene in 50/50 mixtures is reduced slightly compared to the pure component isotherm of propene. Both the simulations and the IAST suggest a reversal of the selectivity at very high pressure. The adsorption of benzene in the 50/50 mixture is almost identical to the

adsorption of the pure component isotherm. This suggests that in contrast to zeolites BEA, MCM22, FAU, and MOR propene is adsorbed at different adsorption sites inside the zeolite. Simulation snapshots show that benzene is preferentially adsorbed at the intersections and that propene can adsorb at both the intersections and the channel interiors (Figure 12a). In the presence of benzene, the intersections are occupied by the stronger adsorbing benzene molecules, and therefore propene is exclusively adsorbed in the channel interiors (Figure 12b), resulting in a somewhat lower adsorption of propene compared to the pure component isotherm.

Figure 6b showed that at 373 K the selectivity for benzene is even reversed in favor of propene. The reason is that at a total pressure of 1 bar the loading of benzene is limited by the number of channel intersections. Therefore, as soon as the intersections are filled with benzene, increasing the partial pressure of benzene does not result in a higher loading of benzene, so the $x-y$ diagram will be quite flat for a large range of partial pressures of benzene. This effect will be more pronounced at low temperatures. At higher temperatures, the total loading of benzene is lower than four molecules per unit cell and therefore this effect does not play a role.

4. Conclusions

We have constructed a nine-site force field for the adsorption of benzene in zeolites. The comparison with experimental data revealed a good agreement with our simulations. The selectivity for benzene in benzene/propene mixtures is investigated for various zeolites that have the potential to be used as catalysts for cumene synthesis. High selectivities for benzene are found in zeolite β, MCM22, and MOR. The selectivity of these zeolites is hardly influenced by temperature. Silicalite is not very selective for benzene. Zeolite Y is an intermediate case because the selectivity for benzene is low at low partial pressures and high temperatures. A lower temperatures, however, the selectivity for benzene is high at sufficiently high pressure.

Acknowledgment. We thank Marcel Janssen and Sebastien Kremer (ExxonMobil) for providing the silicalite sample and the SEM image. We thank Krijn de Jong for fruitful discussions. We acknowledge funding from the ACTS/ASPECT program from The Netherlands Organization for Scientific Research (NWO-CW). T.J.H.V. acknowledges financial support from NWO through a VIDI grant, and P.E.d.J. acknowledges financial support from NWO through a MEERVOUD grant.

References and Notes

(1) Meima, G. R.; van der Aalst, M. J. M.; Samson, M. S. U.; Graces, J. M.; Lee, J. G. *EDRÖL ERDGAS KOHLE* **1996**, *7*, 315.

(2) de Jong, K. P.; Mesters, C. M. A. M.; Peferoen, D. G. R.; Brugge, P. T. M.; Groot, C. *Chem. Eng. Sci*. **1996**, *51*, 2053−2060.

(3) Meima, G. R. *Cattech* **1998**, *2*, 5−12.

(4) Stach, H.; Lohse, U.; Thamm, H.; Schirmer, W. *Zeolites* **1986**, *6*, 74−90.

(5) Sun, M. S.; Talu, O.; Shah, D. B. *J. Phys. Chem.* **1996**, *100*, 17276−17280.

(6) Zhu, W.; van de Graaf, J. M.; van den Broeke, L. J. P.; Kapteijn, F.; Moulijn, J. A. *Ind. Eng. Chem. Res.* **1998**, *37*, 1934−1942.

(7) van Donk, S.; Broersma, A.; Gijzeman, O. L. J.; van Bokhoven, J. A.; Bitter, J. H.; de Jong, K. P. *J. Catal*. **2001**, *204*, 272−280.

(8) Arik, I. C.; Denayer, J. F. M.; Baron, G. V. *Microporous Mesoporous Mater*. **2003**, *60*, 111−114.

(9) van Donk, S.; Bitter, J. H.; Verberckmoes, A.; Versluis-Helder, M.; Broersma, A.; de Jong, K. P. *Angew. Chem., Int. Ed.* **2005**, *44*, 1360−1364.

(10) Smit, B.; Siepmann, J. I. *Science* **1994**, *264*, 1118−1120.

(11) Vlugt, T. J. H.; Krishna, R.; Smit, B. *J. Phys. Chem. B* **1999**, *103*, 1102−1118.

(12) Krishna, R.; Paschek, D. *Phys. Chem. Chem. Phys.* **2001**, *3*, 453−462.

(13) Krishna, R.; Smit, B.; Calero, S. *Chem. Soc. Rev.* **2002**, *31*, 185−194.

(14) Pascual, P.; Ungerer, P.; Tavitian, B.; Pernot, P.; Boutin, A. *Phys. Chem. Chem. Phys.* **2003**, *5*, 3684−3693.

(15) Dubbeldam, D.; Calero, S.; Vlugt, T. J. H.; Krishna, R.; Maesen, T. L. M.; Smit, B. *J. Phys. Chem. B* **2004**, *108*, 12301−12313.

(16) Calero, S.; Dubbeldam, D.; Krishna, R.; Smit, B.; Vlugt, T. J. H.; Denayer, J. F. M.; Martens, J. A.; Maesen, T. L. M. *J. Am. Chem. Soc.* **2004**, *126*, 11377−11386.

(17) Jakobtorweihen, S.; Hansen, N.; Keil, F. J. *Mol. Phys.* **2005**, *103*, 471−489.

(18) Maginn, E. J.; Bell, A. T.; Theodorou, D. N. *J. Phys. Chem.* **1995**, *99*, 2057−2079.

(19) Macedonia, M. D.; Maginn, E. J. *Mol. Phys.* **1999**, *96*, 1375−1390.

(20) Macedonia, M.D.; Maginn, E. J. *Fluid Phase Equilib.* **1999**, *160*, 19−27.

(21) Pascual, P.; Ungerer, P.; Tavitian, B.; Boutin, A. *J. Phys. Chem. B* **2004**, *108*, 393−398.

(22) Snurr, R. Q.; Bell, A. T.; Theodorou, D. R. *J. Phys. Chem.* **1993**, *97*, 13742−13752.

(23) Jorgensen, W. L.; Severance, D. L. *J. Am. Chem. Soc.* **1990**, *112*, 4768−4774.

(24) Chempath, S.; Snurr, R. Q.; Low, J. J. *AIChE J.* **2004**, *50*, 463−469.

(25) Yue, X. P.; Yang, X. N. *Langmuir* **2006**, *22*, 3138−3147.

(26) Zeng, Y. P.; Ju, S. G.; Xing, W. H.; Chen, C. L. *Ind. Eng. Chem. Res.* **2007**, *46*, 242−248.

(27) Baker, C. M.; Grant, G. H. *J. Chem. Theory Comput.* **2006**, *2*, 947−955.

(28) Zhao, X. S.; Chen, B.; Karaborni, S.; Siepmann, J. I. *J. Phys. Chem. B* **2005**, *109*, 5368−5374.

(29) Janda, K. C. *J. Chem. Phys.* **1975**, *63*, 1419.

(30) Steed, J. M. *J. Chem. Phys.* **1979**, *70*, 4940.

(31) Arunan, E.; Gutowsky, H. S. *J. Chem. Phys.* **1993**, *98*, 4294−4296.

(32) Wick, C. D.; Siepmann, J. I.; Klotz, W. L.; Schure, M. R. *J. Chromatogr., A* **2002**, *954*, 181−190.

(33) Smit, B. *Mol. Phys.* **1995**, *85*, 153−172.

(34) Smit, B. *J. Phys. Chem.* **1995**, *99*, 5597−5603.

(35) Frenkel, D.; Smit, B. *Understanding Molecular Simulation: from Algorithms to Applications*, 2nd ed; Academic Press: San Diego, CA, 2002.

(36) Wood, G. B.; Panagiotopoulos, A. Z.; Rowlinson, J. S. *Mol. Phys.* **1988**, *63*, 49−63.

(37) van Koningsveld, H.; Tuinstra, F.; van Bekkum, H.; Jansen, J. C. *Acta Crystallogr.* **1989**, *B45*, 423−431.

(38) Meier, W. M.; Olson, D. H.; Baerlocher, Ch. *Atlas of Zeolite Structure Types*, 4th ed.; Elsevier: Amsterdam, 1996.

(39) Vlugt, T. J. H.; Schenk, M. *J. Phys. Chem. B* **2002**, *106*, 12757−12763.

(40) Jorgensen, W. L.; Madura, J. D.; Swenson, C. J. *J. Am. Chem. Soc.* **1984**, *106*, 6638−6646.

(41) Chen, D.; Rebo, H. P.; Moljord, K.; Holmen, A. *Chem. Eng. Sci.* **1996**, *51*, 2687−2692.

(42) Peng, J.; Ban, H. Y.; Zhang, X. T.; Song, L. J.; Sun, Z. L. *Chem. Phys. Lett.* **2005**, *401*, 94−98.

(43) Thamm, H.; Stach, H.; Berezin, G. I. *Z. Chem.* **1984**, *24*, 420.

(44) Breck, D. W. *Zeolite Molecular Sieves*; Wiley: New York, 1974.

(45) Talu, O.; Guo, C. J.; Hayhurst, D. T. *J. Phys. Chem.* **1989**, *93*, 7294−7298.

(46) Olsen, D. H.; Kokotailo, G. T.; Lawton, S. L.; Meier, W. M. *J. Phys. Chem.* **1981**, *85*, 2238−2243.

(47) Lee, C. K.; Chiang, A. S. T.; Wu, F. Y. *AIChE J.* **1992**, *38*, 128−135.

(48) Song, L.; Sun, Z. L.; Ban, H. Y.; Dai, M.; Rees, L. V. C. *Adsorption* **2005**, *11*, 325−339.

(49) Fyfe, C. A.; Feng, Y.; Grondey, H.; Kokotailo, G. T. *Chem. Soc. Chem. Commun.* **1990**, *18*, 1224−1226.

(50) Portsmouth, R. L.; Duer, M. J.; Gladden, L. F. *J. Chem. Soc., Faraday Trans.* **1995**, *93*, 559−567.

(51) Vlugt, T. J. H.; Zhu, W.; Kapteijn, F.; Moulijn, J. A.; Smit, B.; Krishna, R. *J. Am. Chem. Soc.* **1998**, *120*, 5599−5600.

(52) Wu, P. D.; Debebe, A.; Ma, Y. H. *Zeolite* **1983**, *3*, 118.

(53) Jentys, A.; Mukti, R. R.; Tanaka, H.; Lercher, J. A. *Microporous Mesoporous Mater.* **2006**, *90*, 284−292.

(54) Pope, C. G. *J. Phys. Chem.* **1986**, *90*, 835−837.

(55) Takahashi, A.; Yang, F. H.; Yang, R. T. *Ind. Eng. Chem. Res.* **2002**, *41*, 2487−2496.

(56) Myers, A. L.; Prausnitz, J. M. *AIChE J.* **1965**, *11*, 121−130.

(57) Murthi, M.; Snurr, R. Q. *Langmuir* **2004**, *20*, 2489−2497.